

## Highlights

### **Deep learning for chemical kinetic modeling in ammonia-methane combustion with a posteriori validation**

Ke Xiao, Yangchen Xu, Han Li, Zhi X. Chen

- DNN models replace direct integration of NH<sub>3</sub>/CH<sub>4</sub> chemical kinetics.
- Data augmentation based on flame structure physics improves training data quality.
- DNNs demonstrate strong predictive accuracy in unseen flame scenarios.
- Up to 20× acceleration in combustion modeling is achieved.

# Deep learning for chemical kinetic modeling in ammonia-methane combustion with a posteriori validation

Ke Xiao<sup>a,b</sup>, Yangchen Xu<sup>a,b</sup>, Han Li<sup>a,b,\*</sup>, Zhi X. Chen<sup>a,b</sup>

<sup>a</sup>*State Key Laboratory of Turbulence and Complex Systems, College of Engineering,  
Peking University, Beijing 100871, China*

<sup>b</sup>*AI for Science Institute (AISI), Beijing 100080, China*

---

## Abstract

Deep learning has shown considerable potential for alleviating the primary computational bottleneck in combustion simulations: the direct integration of stiff chemical ordinary differential equations (ODEs) in chemical kinetic modeling. This study investigates the application of deep neural networks (DNNs) as surrogate models for chemical kinetics in ammonia–methane combustion. Thermochemical training data are generated through manifold sampling of one-dimensional (1D) freely propagating premixed laminar flames. To address data imbalance near the flame front, where steep temperature gradients are present, a hybrid interpolation and randomization-based data augmentation strategy is introduced to enrich underrepresented regions in the training dataset. This refinement enhances model accuracy in 1D laminar flame validation tests. Furthermore, *a posteriori* evaluation in a two-dimensional (2D) propagating flame under homogeneous isotropic turbulence

---

\*Corresponding author

Email address: han\_li@pku.edu.cn (Han Li)

(HIT) demonstrates that the trained DNN models retain predictive accuracy under previously unseen conditions while achieving up to a  $20\times$  overall speedup in computational performance. These results highlight the potential of DNN-based chemical kinetics to accelerate ammonia combustion modeling, supporting more efficient and scalable high-fidelity simulations for practical applications.

*Keywords:* Deep learning, Chemical kinetics, Ammonia-methane blends, Combustion modeling

---

## 1. Introduction

Ammonia has gained significant attention as a carbon-free fuel and hydrogen carrier [1, 2, 3, 4], aligning with the United Nations' Sustainable Development Goals (SDGs), which aim to pursue sustainable energy solutions that are accessible, reliable, and environmentally friendly. Key benefits of ammonia as a fuel include its zero carbon content, high volumetric energy density, and an established infrastructure for production, storage, and transport [5, 6]. However, challenges such as low flammability, low radiation intensity, and high  $\text{NO}_x$  emissions due to its nitrogen content necessitate further research to enhance ammonia combustion. Significant efforts have focused on blending ammonia with highly reactive fuels, such as hydrogen, methane, syngas, and dimethyl ether, to improve overall combustion properties like burning velocity and adiabatic flame temperature, thus enabling the use of ammonia in existing combustion systems with minimal modifications [7].

Numerical simulations are crucial for understanding the complex interac-

tions in ammonia-based fuel blends and optimizing their combustion characteristics. To achieve this, detailed finite-rate chemistry models are essential, as they provide more fundamental insights into combustion phenomena, particularly for ammonia-fueled systems, where flame instability dynamics can be pronounced [8]. However, incorporating detailed chemical kinetics significantly increases computational costs, especially in simulations involving ammonia blends, where comprehensive chemical mechanisms typically consist of dozens of species [9]. Description of chemistry using these mechanisms requires direct integration of stiff systems of ordinary differential equations (ODEs) that govern species concentration evolution. The stiffness, stemming from the wide range of chemical timescales, necessitates extremely small time steps for stable and accurate integration, thereby making the process highly computationally demanding. In practical simulations, chemistry evaluation alone can account for over 90% of total computational time, posing a major bottleneck in high-fidelity combustion modeling.

Recently, machine learning techniques for accelerating chemistry-related computations have gained increasing interest [10, 11, 12, 13]. Deep learning, a subset of machine learning utilizing deep neural networks (DNNs) to model complex patterns in large datasets, has been applied in combustion simulations as an alternative to traditional ODE integrators. By framing the integration process as a regression problem—predicting changes in species concentrations over time based on initial conditions—deep learning models can approximate chemical source terms without the need for stiff ODE integration at each time step. This approach can also be viewed as a form of data storage and retrieval or tabulation, as DNNs learn patterns from extensive

datasets of precomputed chemistry calculations and perform inference with new, unseen data during simulations [14, 15].

Compared to traditional tabulation methods, DNNs avoid the need for dimension reduction, which can compromise accuracy. They typically require significantly less memory [16], since they only need to store a set of model parameters and weights instead of input-output pairs. Furthermore, DNN inference benefits from modern Graphics Processing Units (GPUs), optimized for parallel computation, which enables rapid processing of multiple inputs simultaneously. This greatly enhances inference speed and makes real-time evaluations feasible in complex chemical systems. However, challenges such as data curation, model selection, evaluation, and validation remain significant hurdles, limiting the broader application of this methodology.

Addressing these hurdles begins with the creation of high-quality training datasets, since the effectiveness and reliability of DNN-based chemistry models directly depend on the representativeness of their data. Due to the limited extrapolation capabilities of data-driven methods, researchers have focused on constructing datasets that encompass thermochemical states representative of those encountered in later combustion simulations. For instance, An et al. [17] sampled data from a Reynolds-Averaged Navier-Stokes (RANS) pre-simulation and applied their models in Large Eddy Simulations (LES) of the same problem, while Chi et al. [18] utilized on-the-fly training in Direct Numerical Simulations (DNS) to ensure that the training data is representative of inference data.

While problem-specific sampling from the target case ensures high fidelity, it often limits the generalizability and reusability of DNN-based chemistry

models across diverse scenarios. To address this, researchers have adopted generic canonical problem sampling, leveraging fundamental reacting-flow configurations to generate broadly representative thermochemical datasets. For example, Wan et al. [19] sampled data from turbulent, non-adiabatic, non-premixed micro-mixing canonical problems and applied the trained neural networks to DNS of a syngas turbulent oxy-flame. Similar configurations were also used by Béroudiaux et al. [20] for modeling high-pressure hydrogen–air combustion. Chatzopoulos and Rigopoulos [21] extracted data from non-premixed flamelets at varying strain rates for RANS-PDF simulations of  $\text{CH}_4/\text{H}_2/\text{N}_2$  turbulent flames, a low-dimensional manifold sampling methodology further expanded by Franke et al. [22], Ding et al. [15], and Readshaw et al. [23]. Such approaches have also been explored to create initial databases for other storage and retrieval methods by Newale et al. [24]. They demonstrated that both flamelets and partially stirred reactor (PaSR) simulations can effectively generate representative thermochemical states encountered in combustion simulations. The core idea behind these generic canonical problem sampling methods is that, under the same initial working conditions, ensembles of thermochemical states throughout the evolution of chemical systems form a continuous manifold [25].

Despite recent progress, the data preparation process for DNN-based chemical kinetics remains a non-trivial challenge. Constructing large, high-quality datasets that accurately capture the complex thermochemical states encountered in reactive flows is critical yet difficult, particularly for fuels with intricate chemical behavior. Notably, most existing studies in this area have concentrated on hydrocarbon fuels with relatively simplified mechanisms.

In contrast, ammonia combustion introduces additional complexity due to nitrogen-bearing species and a wide spectrum of chemical time scales, which significantly complicate both data generation and model learning. To date, limited efforts have been made to extend DNN-based surrogate models to ammonia-fueled systems.

To address these gaps, this study explores deep learning–based chemical kinetics modeling for NH<sub>3</sub>/CH<sub>4</sub> combustion using the comprehensive mechanism by Okafor et al. [26], comprising 59 species and 356 elementary reactions. Thermochemical training data are generated from canonical one-dimensional premixed laminar flames, and a physics-aware data augmentation strategy is introduced to improve coverage in underrepresented regions, particularly near steep thermochemical gradients. The trained models are first validated in 1D laminar flames and subsequently evaluated *a posteriori* in a two-dimensional homogeneous isotropic turbulence (HIT) flame configuration to assess generalizability and computational performance. This study advances the application of deep neural networks to ammonia-fueled combustion and presents a scalable framework for accelerating high-fidelity simulations involving complex chemical kinetics.

## 2. Methodology

### 2.1. Deep learning for combustion chemistry integration

A chemical system with  $N$  species and  $M$  reactions can be expressed as:

$$\sum_{\alpha=1}^N \nu'_{\alpha j} \mathcal{M}_\alpha \Rightarrow \sum_{\alpha=1}^N \nu''_{\alpha j} \mathcal{M}_\alpha \quad \text{for } j = 1, \dots, M, \quad (1)$$

Here,  $\mathcal{M}_\alpha$  denotes species  $\alpha$ , while  $\nu'_{\alpha j}$  and  $\nu''_{\alpha j}$  represent the molar stoichiometric coefficients for species  $\alpha$  in reaction  $j$ . The reaction rate of species  $\alpha$  is described by the following ODE:

$$\frac{dY_\alpha}{dt} = W_\alpha \sum_{j=1}^M (\nu'_{\alpha j} - \nu''_{\alpha j}) \left\{ K_{fj} \prod_{\alpha=1}^N \left( \frac{\rho Y_\alpha}{W_\alpha} \right)^{\nu'_{\alpha j}} - K_{rj} \prod_{\alpha=1}^N \left( \frac{\rho Y_\alpha}{W_\alpha} \right)^{\nu''_{\alpha j}} \right\} \quad (2)$$

where  $Y_\alpha$  is the mass fraction and  $W_\alpha$  is the molecular weight of species  $\alpha$ . The mixture mass density is represented by  $\rho$ , while  $K_{fj}$  and  $K_{rj}$  are the forward and reverse rate constants for reaction  $j$ . These rate constants are typically parameterized by temperature  $T$  according to Arrhenius models and also pressure  $p$  for pressure-dependent reaction rates.

For simulation methods that require real-time computation of the chemical source term in every grid cell and time step, the source terms  $\dot{\omega}_\alpha$  are obtained through time integration of the ODE system mentioned above. This process could be replaced by DNN surrogate models that fit the nonlinear mapping functions between input-output pairs.

As shown in Equation 2, in combustion processes characterized by incompressible or weakly compressible flows, the instantaneous reaction source terms  $\dot{\omega}_\alpha$  can be expressed as a function of  $T$ ,  $p$  and the mass fraction vector  $\mathbf{Y} = (Y_1, Y_2, \dots, Y_N)$ . Therefore, the input chosen for the neural networks are local thermochemical parameters  $\{T(t), p(t), \mathbf{Y}(t)\}$ , and the outputs are  $\{\mathbf{Y}(t + \Delta t) - \mathbf{Y}(t)\}$ , which are further used to calculate chemical source terms provided for the governing PDEs of the reacting flow systems. Figure 1 illustrates the training process of DNN models and their integration with

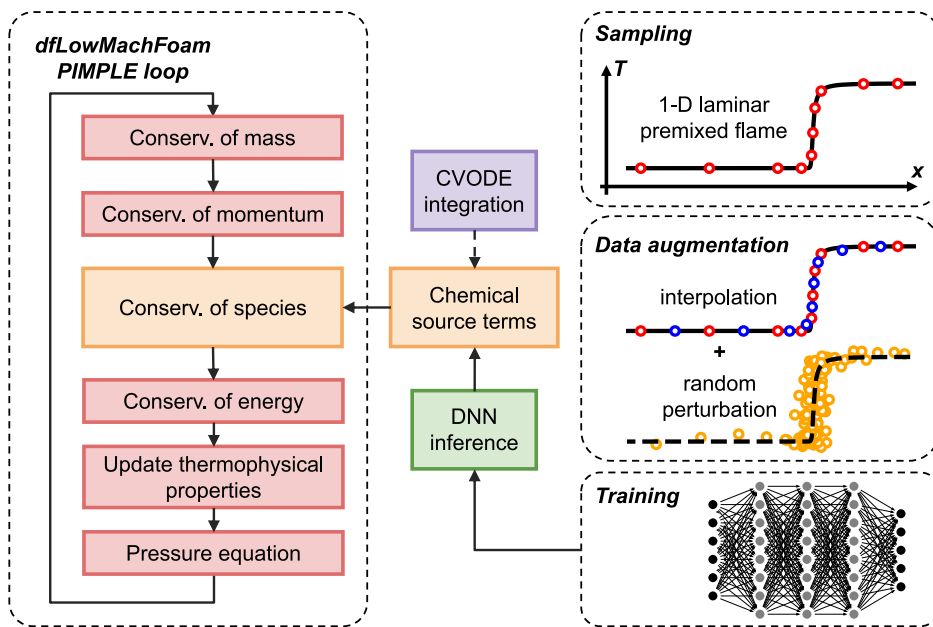


Figure 1: Overview of the training procedure and flow chart for the dfLowMachFoam solver, illustrating the integration of DNN models to provide chemical source terms.

reacting flow solvers. The training process starts with the collection of input datasets, which are then fed into the DNN architecture consisting of an input layer, multiple hidden layers, and an output layer. Throughout the training phase, the DNN develops the ability to accurately map input parameters to desired outputs. This is achieved through the optimization of a loss function that measures the difference between the predicted outputs and the actual results generated by the CVODE integrators from SUNDIALS, as provided by Cantera [27].

Once trained, the DNN is coupled with the dfLowMachFoam solver from the open-source reacting flow simulation platform DeepFlame [28]. This solver computes the flow field and local conditions of the reacting mixture. At each time step, dfLowMachFoam retrieves the current simulation values and inputs them into the DNN for inference. The DNN then predicts reaction rates, which are incorporated into the conservation equations of species. Further details can be found in previous works [29].

## *2.2. Thermochemical base state collection*

Data-driven models, particularly DNNs, heavily depend on the quality of their training data and often struggle with unseen data due to their limited extrapolation capabilities. For DNN models applied to realistic numerical combustion simulations, it is crucial that the training dataset adequately spans the relevant composition space encountered in real-time applications to ensure robustness and applicability.

To construct a representative training dataset for premixed combustion simulations, thermochemical base states are derived from lower-dimensional canonical flames, specifically one-dimensional freely propagating premixed

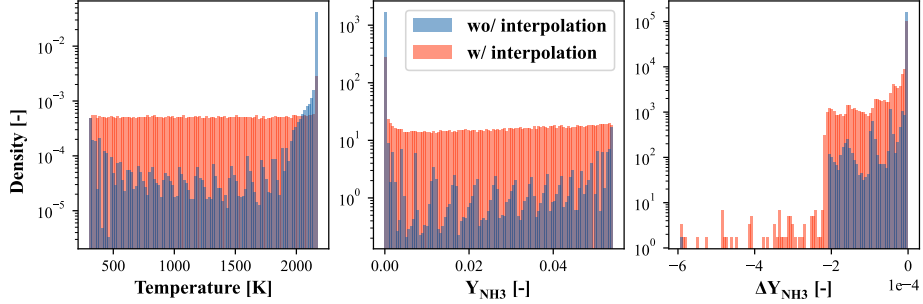


Figure 2: Density distribution of temperature, ammonia mass fraction  $Y_{\text{NH}_3}$ , and deviations in ammonia concentration  $\Delta Y_{\text{NH}_3}$  for datasets with and without interpolation augmentation.

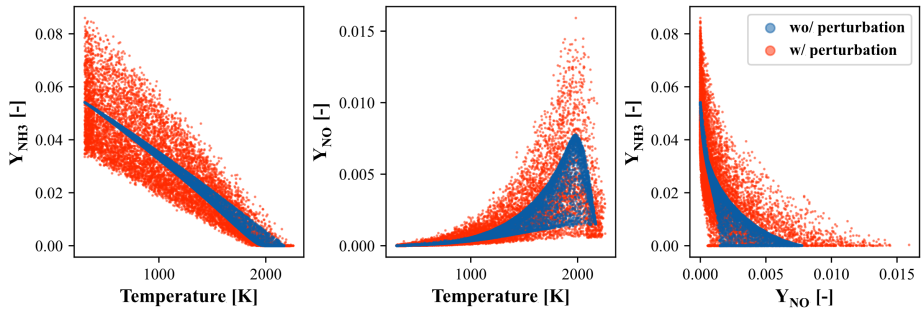


Figure 3: Scatter plots of ammonia mass fraction  $Y_{\text{NH}_3}$ , nitric oxide mass fraction  $Y_{\text{NO}}$  against temperature for datasets with and without perturbation augmentation.

laminar flames. These base states closely resemble realistic turbulent flames with similar fuel and oxidizer compositions, making them an ideal starting point for the training data preparation process.

In this study, we focus on DNN models for a specific  $\text{NH}_3$  blending ratio of 60% and stoichiometric equivalence ratio for  $\text{NH}_3/\text{CH}_4$  mixtures. These models prove to be able to effectively simulate  $\text{NH}_3/\text{CH}_4$  premixed flames with such an  $\text{NH}_3$  blending ratio and equivalence ratio under varying turbu-

lent flow conditions. This choice keeps the data preparation process in the simplest form, which allows for a more manageable complexity and faster training times. The data preparation process can be easily adjusted for different blending and equivalence ratios as needed.

The selection of a 60% NH<sub>3</sub> blending ratio is informed by empirical results, which indicate that models trained at this ratio exhibit reduced performance compared to those trained at lower blending ratios. This decline in performance is likely due to the larger thermochemical composition space associated with the differing reactivity between ammonia and methane at higher blending ratios. Consequently, focusing on a 60% blending ratio allows us to streamline the training process while enhancing model reliability, establishing a solid foundation for future research into more complex configurations.

Although a broader range of blending and equivalence ratios could improve the models' applicability, doing so would necessitate larger datasets and more complex architectures, which might compromise computational efficiency. Thus, this focused approach ensures that we maintain a balance between model performance and practical applicability to real-world scenarios, ultimately facilitating future advancements in this area of research.

To develop a DNN model applicable to turbulent premixed combustion simulations of NH<sub>3</sub>/CH<sub>4</sub> mixtures with a NH<sub>3</sub> blending ratio of 60% and a global equivalence ratio of 1, we sample from a single 1D freely propagating premixed laminar flame. The unburnt gas temperature is set to be 300 K, and the ambient pressure is 1 atm. The computational domain consists of premixed fuel/air mixtures in one half and equilibrium states computed

using Cantera in the other half. The mesh resolution is designed to resolve the flame thickness with 10 grid cells, totaling 500 cells in the simulation domain. The inlet velocity is determined by the laminar flame speed obtained from Cantera to sustain the flame front within the domain.

Simulations are conducted with a fixed time step of  $\Delta t = 1e^{-6}$ s for a duration of 2.5 ms with every time step sampled, resulting in an initial dataset of 1,250,000 states. Without the need to sample from multiple lower-dimensional simulations, the training data generation process becomes straightforward and efficient. The reduced complexity in data generation saves time and computational resources, allowing for quicker iterations in model training and easier expansion of the dataset. Additionally, the dataset is easier to manage, which streamlines the workflow and reduces potential errors.

### *2.3. Data augmentation*

Similarly to the findings of Saito et al. [30] and Chen et al. [31], the initial dataset exhibits a higher density of data at lower reaction rates. This issue of data imbalance could potentially result in suboptimal model performance under certain conditions. While various techniques such as density-weighted sampling [30] and data clustering [32, 33, 31] can help mitigate this issue, we present a data augmentation procedure through interpolation based on physical understanding of 1D laminar flame structure. Unlike density-weighted sampling methods, which filter out data and may exclude rare or extreme conditions, our approach adds new data points without necessitating multiple DNNs to learn from clustered data.

To ensure that adequate thermochemical states at higher reaction rates

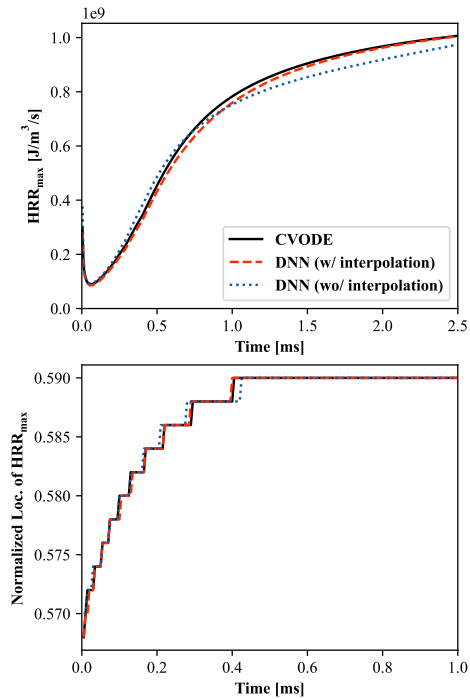


Figure 4: Temporal recordings of the maximum heat release rate (HRR) and the location of the grid cell with the maximum heat release rate, normalized by the simulation domain length.

are included, it is essential to sample more data points from the flame front area. In the case of 1D laminar flames, this region displays significant temperature gradients. Therefore, linear interpolation of other thermochemical properties could be performed based on temperature values to generate additional data points representative of thermochemical conditions within the flame front. For each time step, the 500 thermochemical states are sorted according to temperature, and new states are generated through one-dimensional piecewise linear interpolation of discrete data points ( $T_{init}, f_{init}$ ), where  $T_{init}$  represents the sorted temperatures and  $f_{init}$  is either pressure  $p$  or mass fraction  $Y_\alpha$ . The interpolation is evaluated at points with uniform intervals  $\{T_{new}\}$ .

Figure 2 illustrates the density distribution of temperature, ammonia mass fraction  $Y_{\text{NH}_3}$  and  $\Delta Y_{\text{NH}_3}$  for one dataset with interpolation augmentation and one without. The dataset with interpolation shows a more uniform distribution for all three parameters. The interpolation process balances sampling frequency across different input parameters and improves the training dataset by alleviating data imbalance. This can enable DNN models to generalize better across input ranges, particularly in regions where data points were previously sparse.

Another issue is that the thermochemical states derived from lower-dimensional flames may not fully capture the relevant composition space required for turbulent combustion simulations. They also follow well-defined trajectories within the sample space, making the trained model susceptible to perturbations or deviations from this manifold. To enhance model robustness, data augmentation through random perturbations can simulate multi-dimensional

transport and turbulence effects on the thermochemical structure of the flame, thereby achieving broader coverage of the composition space [15]. In this approach, the original data are discarded in favor of the randomly perturbed data for training, enabling the DNN to learn from points beyond the lower-dimensional flames and improving its applicability to new states.

Both the initial and interpolation-generated states go through random perturbation:

$$T' = T + 100 \cdot X \quad (3)$$

$$p' = p + (\max(p) - \min(p)) \cdot 0.15 \cdot X \quad (4)$$

$$Y'_\alpha = Y_\alpha^{1+0.15 \cdot X} \quad (5)$$

where  $T'$ ,  $p'$ ,  $Y'_\alpha$  represent the perturbed values, and  $X$  is a random number uniformly distributed between -1 and 1. Figure 3 shows the composition space spanned by datasets with and without perturbation augmentation. It is evident that the coverage of the composition space is effectively broadened through random perturbation. However, if left unconstrained, it may produce numerous nonphysical states, which can adversely affect model accuracy in critical regions. Such nonphysical states are primarily observed in areas with higher initial temperatures, corresponding to near-equilibrium states, and demonstrate negative heat release rates of significant magnitude. The perturbation procedure is performed for several rounds, collecting the perturbed data at each iteration. After filtering out the nonphysical states, approximately 8,000,000 valid perturbed states are randomly chosen as the final training dataset.

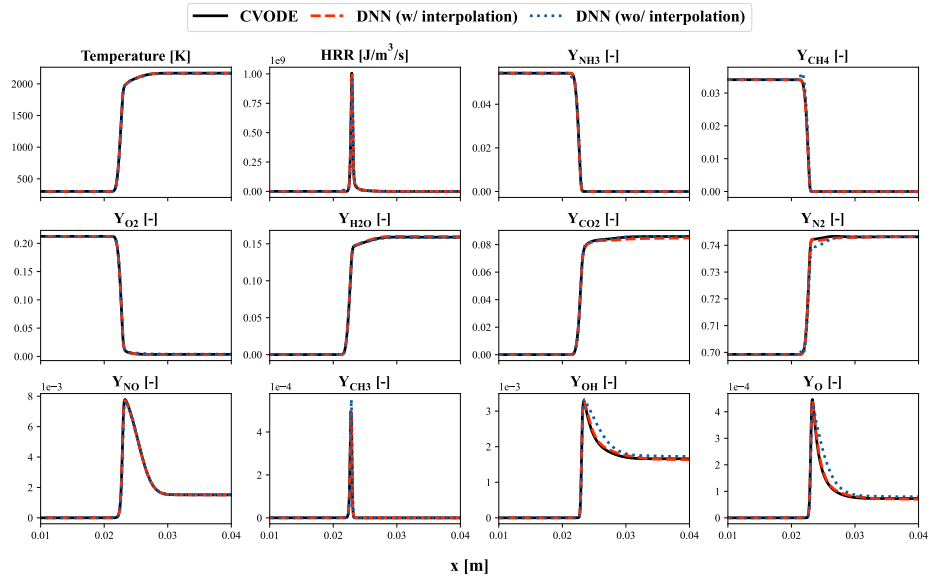


Figure 5: Temperature, heat release rate (HRR), and species mass fractions profiles in physical space obtained at 2.5 ms in 1D laminar premixed flame simulations using DNN inference or CVODE integration for chemical source terms.

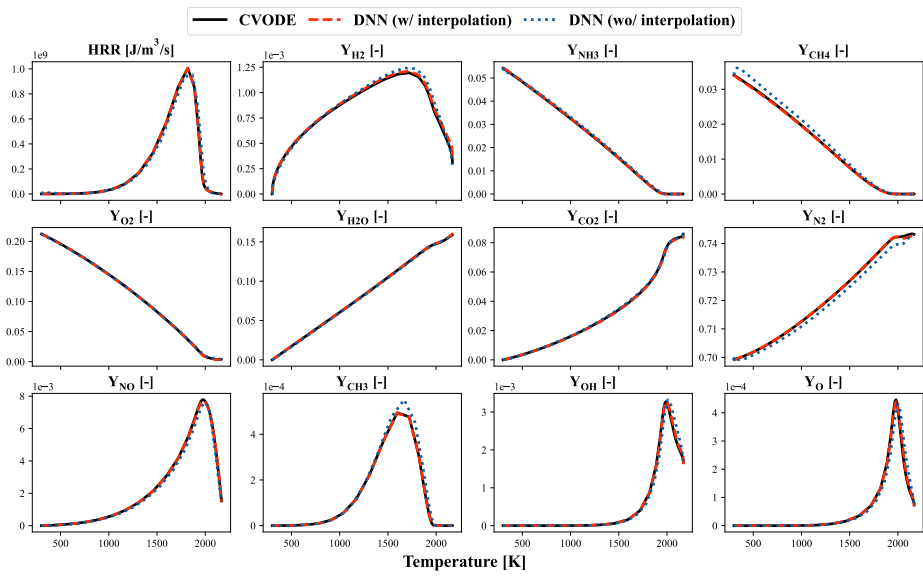


Figure 6: Heat release rate (HRR), and species mass fractions profiles in temperature space obtained at 2.5 ms in 1D laminar premixed flame simulations using DNN inference or CVODE integration for chemical source terms.

#### 2.4. Model architecture and training

The DNN model utilized is a multilayer perceptron (MLP) architecture, comprising an input layer, an output layer, and four hidden layers, each containing 800 neurons. The mass fraction of the inert species argon is excluded from the model output, as it remains constant throughout the reaction process and does not require modeling. The species mass fractions are transformed using the Box-Cox transformation to map data of all magnitudes to a similar scale:

$$\text{BCT}(x) = \frac{x^\lambda - 1}{\lambda} \quad \text{where } \lambda = 0.1 \quad (6)$$

The Box-Cox transformation maps the species mass fractions within the range  $[0, 1]$  to  $[-10, 0]$ . This mapping reduces the non-linearity of the data, which may exhibit very small scales, and provides a more uniform data distribution. The output mass fractions are set as  $\{\text{BCT}(\mathbf{Y}(t+\Delta t)) - \text{BCT}(\mathbf{Y}(t))\}$ . Both the input and output data are normalized using Z-score normalization. Other aspects of the training procedure are consistent with previous studies [29].

#### 2.5. Premixed flame in two-dimensional homogeneous isotropic turbulence

To validate the DNN models in combustion simulations, simulations of a flame kernel ignition of premixed NH<sub>3</sub>/CH<sub>4</sub> mixture in two-dimensional homogeneous isotropic turbulence (HIT) were conducted. Similar setups have been used in previous works [29, 34].

In the simulation, a square computational domain of  $L \times L = 28 \times 28 \text{ mm}^2$  is used, initialized with a premixed stoichiometric mixture of 60%NH<sub>3</sub>/40%CH<sub>4</sub> at 300 K and 1 atm. To ignite the mixture, a circular hot spot with a radius of  $L/10$  filled with equilibrium state gases is placed in the center of

the domain. The HIT generation approach in [35] is adopted and the fully evolved velocity field is then mapped to the computational domain as the initial flow field. Boundary conditions are set to zero gradient for temperature and species mass fractions, and a non-reflective wave transmissive condition is used for pressure and velocity. The domain is uniformly discretized with  $512 \times 512$  grids to ensure sufficient resolution for both flame and turbulence.

### 3. Results

#### 3.1. Application to 1D freely propagating premixed laminar flame

The DNN models are first tested in the 1D freely propagating premixed laminar flame used for training data generation. We compare the results from DNN models trained on datasets with and without interpolation augmentation against simulations using CVODE for chemistry integration.

In Figure 4, the upper panel displays the trajectory of the maximum heat release rate during the simulations. The DNN trained on the dataset with interpolation closely follows the CVODE results, indicating improved accuracy compared to the DNN trained on the dataset without interpolation, which under-predicted reaction intensity. The lower panel illustrates the location of the maximum heat release rate, highlighting flame propagation. Here, the DNN without interpolation exhibits more fluctuating behavior, while the DNN trained with interpolation provides a more stable and accurate prediction of flame location. This improved performance suggests that the DNN trained on the dataset with interpolation is more adept at capturing the dynamics of reactive states. The inaccuracies observed in the DNN without interpolation could lead to significant errors in predicting flame propagation

behavior.

Figure 5 and 6 show the flame structure obtained at 2.5 ms for CVODE and the two DNN models. The results from the DNN models trained on the dataset without interpolation reveal discrepancies in the  $\text{NH}_3$  and  $\text{CH}_4$  profiles on the unburnt side of the flame, as well as in the profiles of intermediate species like  $\text{OH}$  and  $\text{O}$  behind the flame front. These discrepancies are particularly evident in the progress variable space, where a shift in species profiles occurs for the DNN without interpolation. In contrast, the DNN trained on data with interpolation demonstrates better alignment with the CVODE results, indicating superior predictive capability.

### *3.2. Application to premixed flame in two-dimensional homogeneous isotropic turbulence*

The DNN trained on data with interpolation is adopted for the 2D case. We compare the results from DNN inference against simulations using CVODE for chemistry integration. Both simulations are conducted for 4 ms, during which the flame kernel propagates near the boundary. The simulation is then stopped to prevent boundary conditions from producing nonphysical behavior.

Figure 7 illustrates the trajectory of maximum temperature and maximum heat release rate during the simulations. The results from the DNN align well with those obtained from the CVODE simulations for both metrics, with a maximum difference of approximately 5 K in the maximum temperature. This close agreement demonstrates the DNN’s capability to accurately capture the key dynamics of the combustion process. However, it also indicates that there is still room for improvement in prediction accuracy

for equilibrium states, despite the model’s effectiveness in predicting rapidly changing conditions across the flame front.

Several factors may contribute to this behavior. First, the lack of atomic conservation in DNN predictions can lead to discrepancies. Béroudiaux et al. reported that DNNs can diverge when predicting equilibrium states, and that incorporating atomic conservation corrections can effectively address this issue [20]. Although some studies [19, 36] have discussed correction procedures, Béroudiaux et al. [20] emphasized that post-inference corrections do not always yield improved results. It may be more advantageous to integrate atomic conservation directly into the model architecture as hard constraints, as suggested by Rohrhofer et al. in [37].

Another potential reason for the decreased model performance in equilibrium states is the multi-scale nature of combustion chemical kinetics. Rohrhofer et al. [37] et al. highlighted that using loss functions based on absolute errors can result in smaller scale changes being learned less accurately. While the data transformation using Box-Cox transformation in this study may alleviate some multi-scale issues, accuracy problems related to the absolute loss function are likely to persist.

Figure 8 presents calculations of flame area in 2D HIT flame simulations, providing a general description of flame kernel development. The results indicate that the DNN predictions align well with the CVODE results regarding flame area. This reaffirms that the DNN models used in this study possess sufficient accuracy for predicting reacting states, resulting in good agreement with numerical integration methods when capturing flame dynamics.

Figure 9, 10, and 11 show scalar fields of temperature, heat release rate,

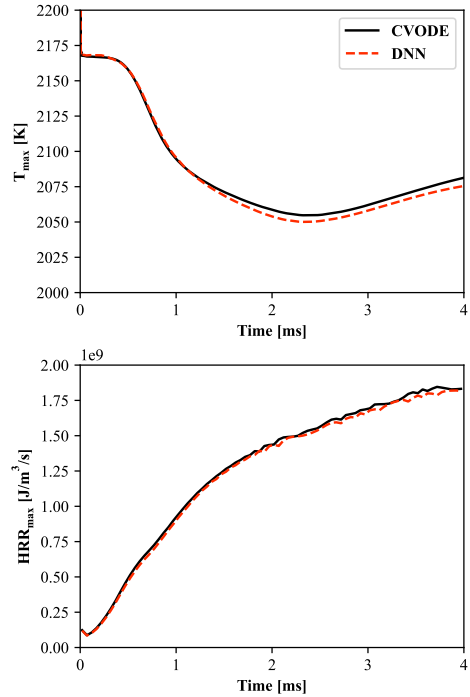


Figure 7: Temporal recordings of the maximum temperature and maximum heat release rate (HRR) in 2D HIT flame simulation.

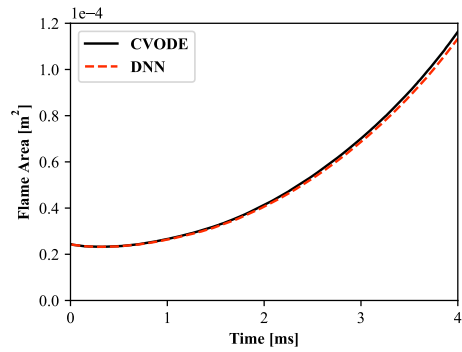


Figure 8: Calculations of flame area in 2D HIT flame simulations.

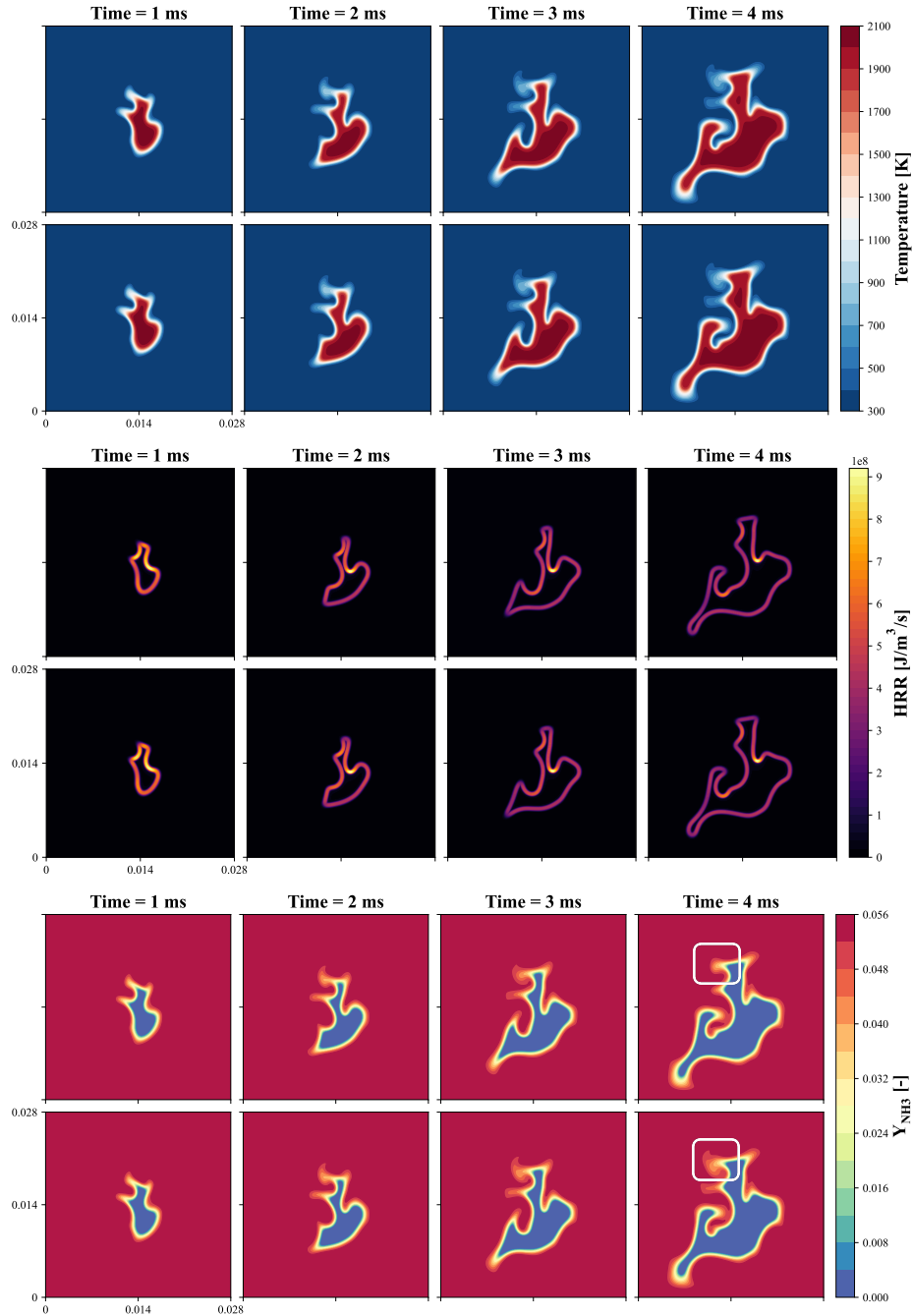


Figure 9: 2D simulations - scalar fields of temperature, heat release rate (HRR), and species mass fractions for  $\text{NH}_3$  ( $Y_{\text{NH}_3}$ ) obtained through DNN (top) and CVODE (bottom).

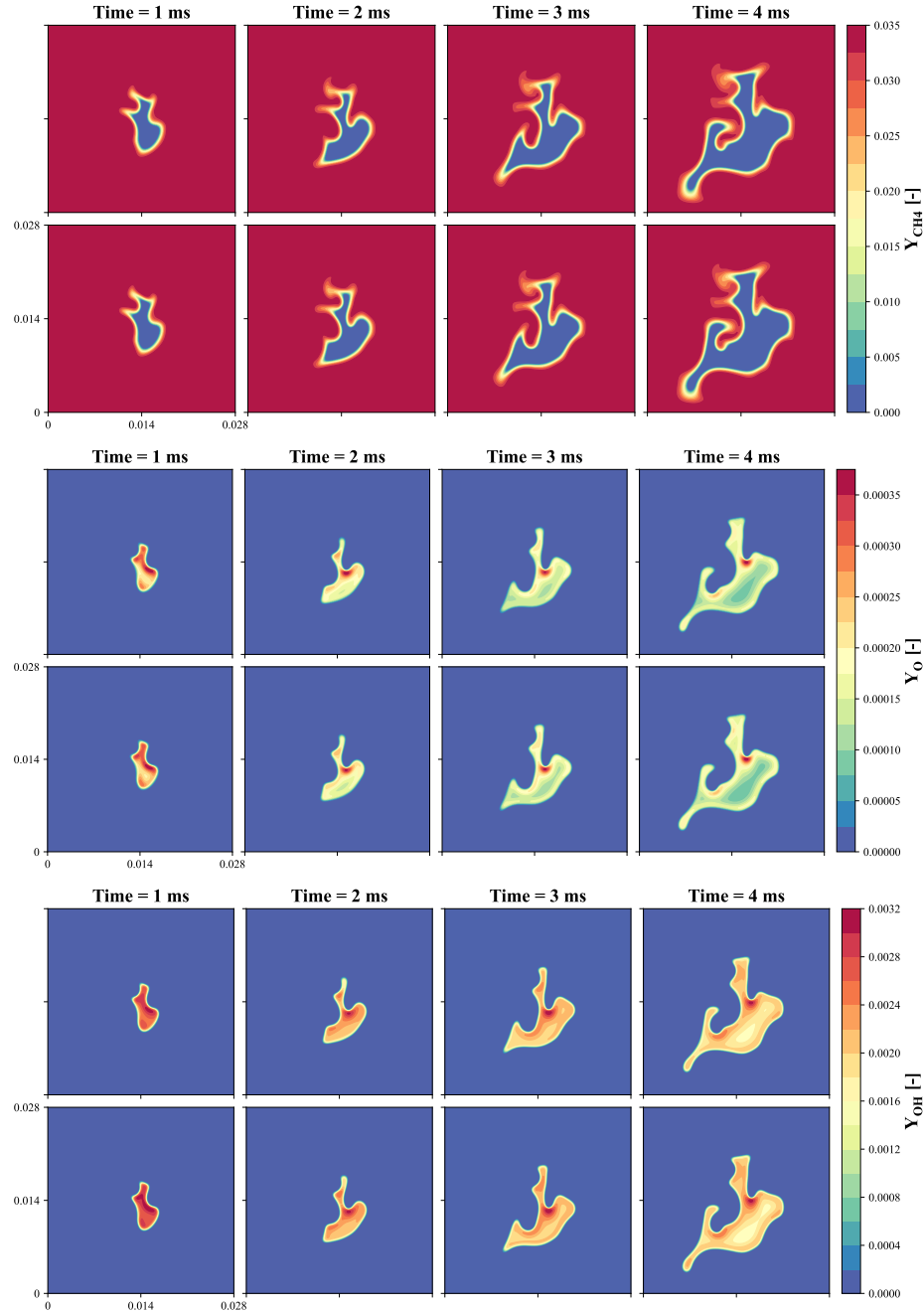


Figure 10: 2D simulations - scalar fields of species mass fractions for  $\text{CH}_4$  ( $Y_{\text{CH}_4}$ ),  $\text{O}$  ( $Y_{\text{O}}$ ), and  $\text{OH}$  ( $Y_{\text{OH}}$ ) obtained through DNN (top) and CVODE (bottom).

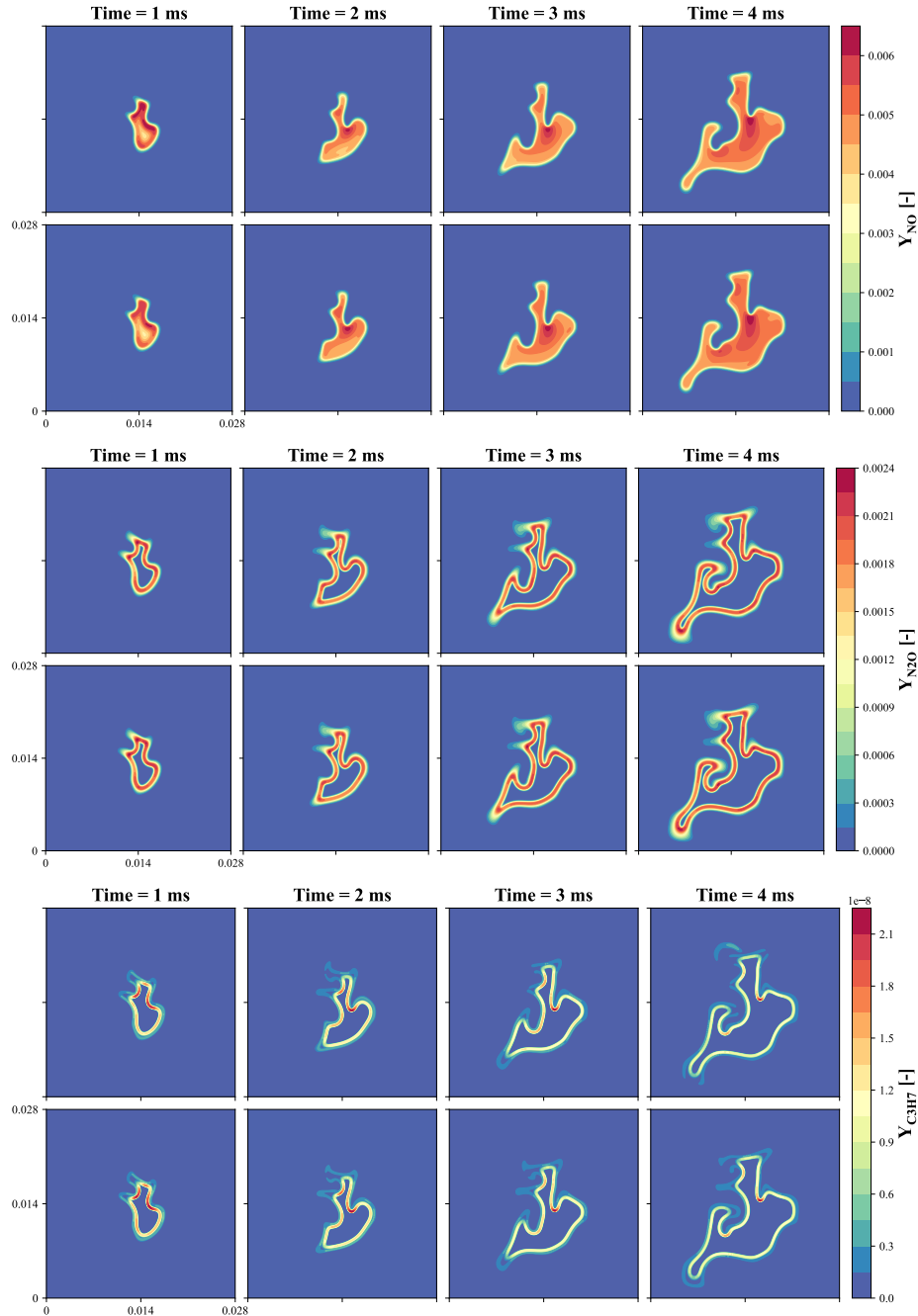


Figure 11: 2D simulations - scalar fields of species mass fractions for NO ( $Y_{NO}$ ), N<sub>2</sub>O ( $Y_{N_2O}$ ), and C<sub>3</sub>H<sub>7</sub> ( $Y_{C_3H_7}$ ) obtained through DNN (top) and CVODE (bottom).

and species mass fractions obtained through DNN and CVODE simulations. The results demonstrate good overall agreement between the DNN and CVODE simulations, indicating that DNN simulations effectively capture the spatial distributions of these quantities throughout iterative model inference and flow field property updates.

Small discrepancies are observed in  $Y_{\text{NH}_3}$  profiles, particularly in the top left corner of the flame at 4 ms. When interpreted in conjunction with the scalar fields of temperature and the mass fractions of other minor species, such as OH, NO, and N<sub>2</sub>O, it becomes evident that the thermochemical composition of this region is predominantly influenced by convection rather than by reaction. This leads to a higher temperature compared to unburnt gases, despite a low heat release rate. Such compositions present challenges for DNN prediction due to the small-scale changes in species composition, similar to the issues encountered in equilibrium states.

Additionally, the differing reactivity between NH<sub>3</sub> and CH<sub>4</sub> may expand the possible composition space, highlighting the need for further exploration of these dynamics to enhance model accuracy and predictive capabilities. Figure 11 presents scalar fields of  $Y_{\text{C}_3\text{H}_7}$ , demonstrating that, at later time steps, discrepancies in  $Y_{\text{C}_3\text{H}_7}$  become larger. CVODE results indicate both production and consumption of C<sub>3</sub>H<sub>7</sub> on the unburnt side of the flame, while DNN simulations fail to capture this behavior accurately.

A similar phenomenon is observed in the 1D laminar premixed flame simulation using Cantera, as indicated by the small secondary peak of  $Y_{\text{C}_3\text{H}_7}$  in Figure 12. To accurately capture such dynamics, it is essential to include related thermochemical compositions in the training data and ensure they are

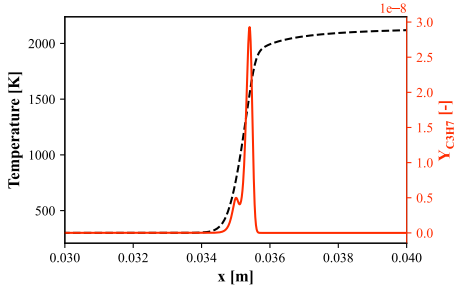


Figure 12: Temperature and  $\text{C}_3\text{H}_7$  mass fraction profiles from 1D freely propagating premixed laminar flame simulated using Cantera.

learned effectively. This underscores the importance of prior knowledge about the chemical kinetic system when developing DNN surrogates for chemistry integration. However, since the species  $\text{C}_3\text{H}_7$  was not included in the sensitivity analysis during mechanism development [26], and considering that important radicals such as O and OH, as well as emission products like NO and  $\text{N}_2\text{O}$  are simulated correctly, the discrepancies in  $Y_{\text{C}_3\text{H}_7}$  can be regarded as acceptable.

The simulations were conducted using 32 Intel Xeon Gold 6330 CPU cores, with an additional 2 NVIDIA GeForce RTX 4090 GPUs used for DNN inference. Compared to previous works [29], data transfer between CPU and GPU has been optimized through data batching, which simplified the process of invoking PyTorch for DNN inference and improved data transfer speed as well as memory consumption, allowing the solver to perform better when processing large-scale data. As a result, DNN simulations achieved a 526 times speedup in chemistry source term calculations. When considering the overall calculation, this translates to a total speedup of 20 times compared to the simulation using CVODE.

## 4. Conclusions

In this work, DNN models were developed as surrogate models for chemistry integration in premixed NH<sub>3</sub>/CH<sub>4</sub> combustion simulations. Training data were generated through simulations of a 1D laminar premixed flame, with data augmentation techniques employed to enhance the dataset. Interpolation was used to increase the number of reacting states, while random perturbation was applied to simulate the effects of turbulence and transport on the thermochemical structure of the flame. These models are intended for application to premixed NH<sub>3</sub>/CH<sub>4</sub> combustion under varying flow conditions, given that the blending ratio and equivalence ratio are the same as the sampled 1D laminar flame.

DNN models trained on datasets with and without interpolation augmentation were tested in 1D laminar flame simulations and compared to results obtained using direct integration through CVODE. The DNN model trained on the interpolated dataset demonstrated superior performance, highlighting the effectiveness of maintaining a balanced training dataset.

In 2D HIT flame simulations, the DNN models achieved a 526 times speedup in chemistry-related calculations, resulting in a total speedup of 20 times compared to CVODE simulations. The DNN predictions for maximum heat release rate and flame area closely aligned with CVODE results. Scalar fields for temperature, heat release rate, and species mass fractions showed good overall agreement, affirming the reliability of the DNN integrator in turbulent combustion simulations.

Limitations of the DNN model in this study are also acknowledged. Enhancements are needed to accurately predict minor species and equilibrium

states, with a significant area for improvement being the inclusion of related thermochemical compositions in the training data. Future work will focus on addressing these limitations and further refining the DNN models to enhance their predictive capabilities in complex combustion scenarios.

## References

- [1] Valera-Medina A, Xiao H, Owen-Jones M, David W, Bowen P. Ammonia for power. *Prog in Energy and Combust Sci.* 2018;69:63–102. <https://doi.org/10.1016/j.pecs.2018.07.001>.
- [2] Valera-Medina A, Amer-Hatem F, Azad A, Dedoussi I, De Joannon M, Fernandes R, et al. Review on Ammonia as a Potential Fuel: From Synthesis to Economics. *Energy & Fuels.* 2021;35(9):6964–7029. <https://doi.org/10.1021/acs.energyfuels.0c03685>.
- [3] Kojima Y, Yamaguchi M. Ammonia as a hydrogen energy carrier. *Int J of Hydrom Energy.* 2022;47(54):22832–22839. <https://doi.org/10.1016/j.ijhydene.2022.05.096>.
- [4] Dimitriou P, Javaid R. A review of ammonia as a compression ignition engine fuel. *Int J of Hydrom Energy.* 2020;45(11):7098–7118. <https://doi.org/10.1016/j.ijhydene.2019.12.209>.
- [5] Yapicioglu A, Dincer I. A review on clean ammonia as a potential fuel for power generators. *Renew and Sustain Energy Rev.* 2019;103:96–108. <https://doi.org/10.1016/j.rser.2018.12.023>.

- [6] Aziz M, Wijayanta A, Nandiyanto A. Ammonia as Effective Hydrogen Storage: A Review on Production, Storage and Utilization. *Energies.* 2020;13(12):3062. <https://doi.org/10.3390/en13123062>.
- [7] Chai W, Bao Y, Jin P, Tang G, Zhou L. A review on ammonia, ammonia-hydrogen and ammonia-methane fuels. *Renew and Sustain Energy Rev.* 2021;147:111254. <https://doi.org/10.1016/j.rser.2021.111254>.
- [8] Lu T, Law C. Toward accommodating realistic fuel chemistry in large-scale computations. *Prog in Energy and Combust Sci.* 2009;35(2):192–215. <https://doi.org/10.1016/j.pecs.2008.10.002>.
- [9] Mikulčić H, Baleta J, Wang X, Wang J, Qi F, Wang F. Numerical simulation of ammonia/methane/air combustion using reduced chemical kinetics models. *Int J of Hydrom Energy.* 2021;46(45):23548–23563. <https://doi.org/10.1016/j.ijhydene.2021.01.109>.
- [10] Meuwly M. Machine Learning for Chemical Reactions. *Chem Rev.* 2021;121(16):10218–10239. <https://doi.org/10.1021/acs.chemrev.1c00033>.
- [11] Zhang T, Yi Y, Xu Y, Chen Z, Zhang Y, E W, et al. A multi-scale sampling method for accurate and robust deep neural network to predict combustion chemical kinetics. *Combust and Flame.* 2022;245:112319. <https://doi.org/10.1016/j.combustflame.2022.112319>.
- [12] Echekki T, Farooq A, Ihme M, Sarathy S. Machine learning for combustion chemistry. In: Machine learning and its application to reacting

flows: ML and combustion. Springer International Publishing Cham; 2023, p. 117–147.

- [13] Ihme M, Chung W. Artificial intelligence as a catalyst for combustion science and engineering. *Proc of the Combust Inst.* 2024;40(1-4):105730. <https://doi.org/10.1016/j.proci.2024.105730>.
- [14] Ren Z, Lu Z, Hou L, Lu L. Numerical simulation of turbulent combustion: Scientific challenges. *Sci China Phys, Mech & Astron.* 2014;57(8):1495–1503. <https://doi.org/10.1007/s11433-014-5507-0>.
- [15] Ding T, Readshaw T, Rigopoulos S, Jones W. Machine learning tabulation of thermochemistry in turbulent combustion: An approach based on hybrid flamelet/random data and multiple multilayer perceptrons. *Combust and Flame.* 2021;231:111493. <https://doi.org/10.1016/j.combustflame.2021.111493>.
- [16] Nikolaou Z, Vervisch L, Domingo P. Criteria to switch from tabulation to neural networks in computational combustion. *Combust and Flame.* 2022;246:112425. <https://doi.org/10.1016/j.combustflame.2022.112425>.
- [17] An J, He G, Luo K, Qin F, Liu B. Artificial neural network based chemical mechanisms for computationally efficient modeling of hydrogen/carbon monoxide/kerosene combustion. *Int J of Hydrog Energy.* 2020;45(53):29594–29605. <https://doi.org/10.1016/j.ijhydene.2020.08.081>.
- [18] Chi C, Janiga G, Thévenin D. On-the-fly artificial neural network for chemical kinetics in direct numerical simulations of

- premixed combustion. *Combust and Flame.* 2021;226:467–477.  
<https://doi.org/10.1016/j.combustflame.2020.12.038>.
- [19] Wan K, Barnaud C, Vervisch L, Domingo P. Chemistry reduction using machine learning trained from non-premixed micro-mixing modeling: Application to DNS of a syngas turbulent oxy-flame with side-wall effects. *Combust and Flame.* 2020;220:119–129.  
<https://doi.org/10.1016/j.combustflame.2020.06.008>.
- [20] Béroudiaux A, Vervisch L, Domingo P. Artificial neural network chemistry solving for high-pressure hydrogen-air combustion. *Int J of Hydrog Energy.* 2025;109:669–683.  
<https://doi.org/10.1016/j.ijhydene.2025.02.054>.
- [21] Chatzopoulos A, Rigopoulos S. A chemistry tabulation approach via Rate-Controlled Constrained Equilibrium (RCCE) and Artificial Neural Networks (ANNs), with application to turbulent non-premixed CH<sub>4</sub>/H<sub>2</sub>/N<sub>2</sub> flames. *Proc of the Combust Inst.* 2013;34(1):1465–1473.  
<https://doi.org/10.1016/j.proci.2012.06.057>.
- [22] Franke L, Chatzopoulos A, Rigopoulos S. Tabulation of combustion chemistry via Artificial Neural Networks (ANNs): Methodology and application to LES-PDF simulation of Sydney flame L. *Combust and Flame.* 2017;185:245–260.  
<https://doi.org/10.1016/j.combustflame.2017.07.014>.
- [23] Readshaw T, Franke L, Jones W, Rigopoulos S. Simulation of turbulent premixed flames with machine learning - tabu-

- lated thermochemistry. *Combust and Flame.* 2023;258:113058. <https://doi.org/10.1016/j.combustflame.2023.113058>.
- [24] Newale A, Sharma P, Pope S, Pepiot P. A feasibility study on the use of low-dimensional simulations for database generation in adaptive chemistry approaches. *Combust Theory and Model.* 2022;26(7):1239–1261. <https://doi.org/10.1080/13647830.2022.2137062>.
- [25] Maas U, Pope S. Simplifying chemical kinetics: Intrinsic low-dimensional manifolds in composition space. *Combust and Flame.* 1992;88(3-4):239–264. [https://doi.org/10.1016/0010-2180\(92\)90034-M](https://doi.org/10.1016/0010-2180(92)90034-M).
- [26] Okafor E, Naito Y, Colson S, Ichikawa A, Kudo T, Hayakawa A, et al. Experimental and numerical study of the laminar burning velocity of CH<sub>4</sub>–NH<sub>3</sub>–air premixed flames. *Combust and Flame.* 2018;187:185–198. <https://doi.org/10.1016/j.combustflame.2017.09.002>.
- [27] Goodwin D, Moffat H, Schoegl I, Speth R, Weber B. Cantera: An Object-oriented Software Toolkit for Chemical Kinetics, Thermodynamics, and Transport Processes. 2022. <https://doi.org/10.5281/ZENODO.6387882>.
- [28] Mao R, Lin M, Zhang Y, Zhang T, Xu Z, Chen Z. DeepFlame: A deep learning empowered open-source platform for reacting flow simulations. *Comput Phys Commun.* 2023;291:108842. <https://doi.org/10.1016/j.cpc.2023.108842>.
- [29] Li H, Yang R, Xu Y, Zhang M, Mao R, Chen Z. Comprehensive deep learning for combustion chemistry integration: Multi-fuel gener-

- alization and *a posteriori* validation in reacting flow. *Phys of Fluids.* 2025;37(1):015162. <https://doi.org/10.1063/5.0248582>.
- [30] Saito M, Xing J, Nagao J, Kurose R. Data-driven simulation of ammonia combustion using neural ordinary differential equations (NODE). *Appl in Energy and Combust Sci.* 2023;16:100196. <https://doi.org/10.1016/j.jaebs.2023.100196>.
- [31] Chen X, Mehl C, Faney T, Di Meglio F. Clustering-Enhanced Deep Learning Method for Computation of Full Detailed Thermochemical States via Solver-Based Adaptive Sampling. *Energy & Fuels.* 2023;37(18):14222–14239. <https://doi.org/10.1021/acs.energyfuels.3c01955>.
- [32] Blasco J, Fueyo N, Dopazo C, Chen J. A self-organizing-map approach to chemistry representation in combustion applications. *Combust Theory and Model.* 2000;4(1):61–76. <https://doi.org/10.1088/1364-7830/4/1/304>.
- [33] Han X, Jia M, Chang Y, Li Y. An improved approach towards more robust deep learning models for chemical kinetics. *Combust and Flame.* 2022;238:111934. <https://doi.org/10.1016/j.combustflame.2021.111934>.
- [34] Cai Y, Yang R, Li H, Xu J, Xiao K, Chen Z, et al. Efficient machine learning method for supercritical combustion: Predicting real-fluid properties and chemical ODEs. *Aerosp Sci and Technol.* 2025;159:110034. <https://doi.org/10.1016/j.ast.2025.110034>.

- [35] Vuorinen V, Keskinen K. DNSLab: A gateway to turbulent flow simulation in Matlab. *Comput Phys Commun*. 2016;203:278–289. <https://doi.org/10.1016/j.cpc.2016.02.023>.
- [36] Readshaw T, Jones W, Rigopoulos S. On the incorporation of conservation laws in machine learning tabulation of kinetics for reacting flow simulation. *Phys of Fluids*. 2023;35(4):047103. <https://doi.org/10.1063/5.0143894>.
- [37] Rohrhofer F, Posch S, Gößnitzer C, García-Oliver J, Geiger B. Utilizing neural networks to supplant chemical kinetics tabulation through mass conservation and weighting of species depletion. *Energy and AI*. 2024;16:100341. <https://doi.org/10.1016/j.egyai.2024.100341>.